Thus, ^{15}N NMR spectroscopy of cyanocobalt corrins enriched in ^{15}N in the axial cyanide proves to be both feasible and extremely instructive. Despite the relatively high sample concentrations required and the relatively long acquistion times needed, such measurements can be made and excellent spectra obtained. Further studies of the inverse dependence of ^{13}C and ^{15}N chemical shifts of cobalt-cyanide species are currently in progress in a simpler model system as well as attempts to observe the ^{15}N NMR spectrum of protein-bound cyanocobalamin.

Acknowledgment. This research was supported by Grant No. DK40212 from the National Institute of Diabetes and Digestive and Kidney Diseases. Purchase of the Bruker MSL 300 NMR spectrometer through a grant from the Defence Advanced Research Projects Agency monitored by the Office of Naval Research is gratefully acknowledged.

(82) Robinson, R. A.; Stokes, R. H. *Electrolyte Solutions*; Butterworths: London, 1959; p 477.

Contribution from the Inorganic Chemistry Laboratory, University of Oxford, South Parks Road, Oxford OX1 3QR, England

Photoelectron Spectroscopy of the Tin Dichalcogenides $SnS_{2-x}Se_x$ Intercalated with Cobaltocene

C. A. Formstone, E. T. FitzGerald, P. A. Cox,* and D. O'Hare

Received November 29, 1989

Single crystals of the n-type semiconducting tin dichalcogenides $SnS_{2-x}Se_x$ (x = 0, 0.3, 0.5, 1.3, 1.85, 2), which have a two-dimensional layered structure, have been intercalated with cobaltocene to give the series of compounds $SnS_{2-x}Se_x(CoCp_2)_{0.33}$, where Cp = η^5-C_5H_5. Photoelectron spectroscopy has been employed to investigate the electronic changes upon intercalation, especially the electron transfer from the guest to the host. X-ray photoelectron spectroscopy (XPS) has revealed mixed oxidation states for both tin [Sn(II), Sn(IV)] and cobalt [Co(I), Co(II), Co(III)]. Of the three cobalt species observed by XPS, two have been unambiguously identified as $CoCp_2$ and $[CoCp_2]^+$, whereas the third cobalt species has only been tentatively assigned to a Co(η^5-C_5H_5)(η^4-C_5H_5R) complex, in which cobalt is formally in the oxidation state Co(I). Ultraviolet photoelectron spectroscopy (UVPES) shows that the intercalates are either semiconducting (x = 0, 0.3, 0.5, 1.3) or metallic (x = 1.85, 2), whereas all the hosts are n-type semiconductors. An impurity-band model is presented as a possible qualitative explanation for this transition through the series.

Introduction

The series of compounds $SnS_{2-x}Se_x$ ($0 < x < 2$) belong to the diverse class of layered materials, which have created interest by virtue of their two-dimensional nature.[1] The crystal structure (space group $P\bar{3}m1$) is similar to that adopted by many transition-metal dichalcogenides (MX_2). It is based upon repeatedly stacked XMX lamellae bound together by van der Waals interactions between adjacent planes of hexagonally closed-packed chalcogenide atoms (X).[2] In SnX_2 the metal atoms are coordinated in nearly octahedral sites.

The process of intercalation by which sheets of guest molecules may be inserted into the interlamellar gaps of the host layered material has been the subject of much research.[3] For example, the search for novel battery systems has led to the development of high-energy-density storage batteries driven by the process of intercalation.[4] In addition, the intercalation of TaS_2 and $TaSe_2$ by a variety of guest species has led to the discovery of a new class of superconductors.[5]

The changes in electronic structure of layered systems upon intercalation can be investigated profitably by using photoelectron spectroscopy (PES).[6,7] For example, a semiconductor to metal transition is induced by the intercalation of K into WS_2.[8] Previous research has indicated that electron transfer occurs between the guest species and host lattice as a result of intercalation.[9] The changes in core- and valence-level electronic structure can provide information on this process and its consequences.[10]

Table I. Growth Conditions, Appearance, and c Spacing for $SnS_{2-x}Se_x$

compn	temp (T_1, T_2), °C	growth time, h	color	c spacing Å
SnS_2	685, 645	12	orange	5.928
$SnS_{1.79}Se_{0.21}$	670, 630	48	red	5.953
$SnS_{1.50}Se_{0.50}$	650, 610	48	dark red	6.008
$SnS_{0.72}Se_{1.28}$	620, 580	100	black	6.103
$SnS_{0.15}Se_{1.85}$	570, 530	50	black	6.136
$SnSe_2$	550, 510	72	black	6.141

The preparation of clean, undisturbed crystal surfaces can be achieved by cleavage of single crystals under ultrahigh vacuum (UHV) within the PES spectrometer. The synthesis of large single crystals (ca. 2 mm × 4 mm) of intercalated materials has often proved difficult. Given the poor kinetics of the general intercalation reaction,[3] the majority of intercalation reactions are only possible with finely powdered host compounds.

This paper describes first the preparation of the series of single crystals $SnS_{2-x}Se_x(CoCp_2)_{0.33}$ (Cp = η^5-C_5H_5, $0 < x < 2$), second their investigation using photoelectron spectroscopy, and third proposal of a qualitative impurity-band-model description of these materials. Cobaltocene intercalation into SnS_2 single crystals has previously been investigated by using X-ray photoelectron spectroscopy.[11] In addition, microcrystalline samples of $SnS_{2-x}Se_x$

(1) Friend, R. H.; Yoffe, A. D. *Adv. Phys.* **1987**, *36*, 1.
(2) Hooter, E., Ed. *Physics and Chemistry of Materials with Layered Structure*; D. Reidel: Dordrecht, The Netherlands, 1976; Vol. 1.
(3) Whittingham, M. S., Jacobsen, A. J., Eds.; *Intercalation Chemistry*; Academic: New York, 1982.
(4) Whittingham, M. S. *Prog. Solid State Chem.* **1978**, *12*, 41.
(5) Gamble, F. R.; DiSalvo, F. J.; Klemm, R. A.; Geballe, T. H. *Science* **1970**, 568.
(6) Eppinga, R.; Sawatsky, G. A.; Haas, C.; von Bruggen, C. F. *J. Phys. C* **1976**, *9*, 3371.
(7) Bach, B.; Thomas, J. M. *J. Chem. Soc., Chem. Commun.* **1972**, 301.
(8) Ohuchi, F. S.; Jaegermann, W.; Pettenkofer, C.; Parkinson, B. A. *Langmuir* **1989**, *5*, 439.
(9) Schöllhorn, R. *Comments Inorg. Chem.* **1983**, *2*, 271.
(10) Briggs, D., Ed. *Handbook of X-ray and Ultraviolet Photoelectron Spectroscopy*; Heyden: London, 1977.
(11) O'Hare, D.; Jaegermann, W.; Williamson, D. L.; Ohuchi, F. S.; Parkinson, B. A. *Inorg. Chem.* **1988**, *27*, 1537.

0020-1669/90/1329-3860$02.50/0

Table II. Stoichiometries, Reaction Conditions, Lattice Expansion, and Appearance for Intercalated Layered Materials $[(host)(CoCp_2)_x]$

host	reacn conditions: temp, °C	reacn conditions: time, days	stoichiometry, x	Δc, Å	color	ref
SnS_2	65	5	0.31	5.46	dark blue	*a*
$SnS_{1.7}Se_{0.3}$	65	7	0.31	5.24	light blue	*a*
$SnS_{1.5}Se_{0.5}$	65	9	0.31	5.20	light blue	*a*
$SnS_{0.7}Se_{1.3}$	65	14	0.33	5.26	black	*a*
$SnS_{0.2}Se_{1.8}$	65	17	0.33	5.50	black	*a*
$SnSe_2$	65	21	0.33	5.56	black	*a*
SnS_2[b]	23	1	0.31	5.55	dark blue	11
$SnSe_2$[b]	125	14	0.33	5.37	black	12
TaS_2[b]	23	24	0.25	5.47	black	3
ZrS_2[b]	100	4	0.27	5.35	black	3

[a] This work. [b] Microcrystalline samples.

$(0 < x < 2)$ have been intercalated with cobaltocene, but no detailed physical study was undertaken by these researchers.[12,13]

Experimental Section

The host single crytals $SnS_{2-x}Se_x$ described in this work were all grown by using the iodine vapor transport method.[14] The high-purity elements (>99.99%) with a 1% molar quantity of phosphorus dopant and the transport agent I_2 (5 mg/cm^3) were sealed in evacuated quartz ampules (10 cm × 1 cm). A three-zone furnace provided a stable temperature gradient between the reaction zone (T_1) and the growth zone (T_2) of the ampule. Table I gives the growth conditions for the various stoichiometries of the series as well as the appearance and *c* spacing of the crystals.

The crystal structure was analyzed by using a Phillips PW 1710 powder diffractometer. The stoichiometry of the host crystals was determined by using a JEOL FX 2000 analytical electron microscope.[15] The X-ray emission from microcrystalline samples excited by a 200-keV electron beam was detected, and the end members of the series were used as standards for the stoichiometry determination.

The synthesis and manipulation of air-sensitive $SnS_{2-x}Se_x(CoCp_2)_{0.33}$ single crystals were carried out under an atmosphere of dinitrogen. The acetonitrile solvent used was predried over molecular sieves and then distilled over CaH_2, followed by thorough degassing.

The crystalline host (ca. 100 mg) was added to a solution of freshly sublimed $CoCp_2$ (ca. 150 mg) in acetonitrile (ca. 5 cm^3). The reaction was carried out at ca. 65 °C without stirring in order to avoid damage to the brittle crystals. After the reaction was complete, typically 5–21 days, the $CoCp_2$ solution was removed and the intercalate washed with acetonitrile (4 × 20 cm^3) until the filtrate was colorless. The single crystals were then dried under vacuum for several hours and characterized by X-ray diffraction under an N_2 atmosphere within a sealed cell. The product crystals were deemed to be fully intercalated when all the host reflections had disappeared from the spectrum. Table II shows the lattice expansion, stoichimetries, appearance, and reaction conditions for the intercalates produced in this study as well as those described in some other papers. The stoichiometry in each case was determined by elemental microanalysis.

The PES measurements were carried out on a VG ESCALAB 5 multichamber spectrometer capable of X-ray photoelectron spectroscopy (XPS), ultraviolet photoelectron spectroscopy (UPS), and low-energy electron diffraction (LEED). The resolution of the unmonochromated X-rays (Mg/Al twin anode) as determined from evaporated gold samples was 1.2 eV. All XPS data were fitted to Gaussian line shapes. The resolution of ultraviolet radiation (~180 meV) was much less than the width of valence-band emissions. The spectrometer was calibrated to take all measurements of binding energy relative to the Fermi level of metallic samples (BE = 0.0 eV).

Single crystals of each sample were pressed into indium foil, previously wrapped around a nickel sample mount. The air-sensitive intercalates were manipulated in an N_2-filled glovebox and then transferred to the spectrometer via a purpose-built transfer device, which could be directly attached to the fast-entry chamber of the spectrometer. Fresh van der Waals faces (001) were produced by cleaving crystals under UHV with the use of small pieces of masking tape. The sample was allowed to degas in the preparation chamber (1 × 10^{-8} mbar) overnight and then transferred immediately after cleavage to the main spectroscopy chamber (5 × 10^{-11} mbar). The host surfaces were deemed to be clean and regular by a combination of XPS and LEED, respectively. Cleaved host crystals gave sharp, hexagonal (1 × 1) LEED patterns over the entire crystal surface. The intercalated samples did not degas CH_3CN into the main chamber. Neither N(1s) nor O(1s) signals were detectable.

Table III. Summary of the Important XPS Binding Energy (eV) Values for the Host and Intercalate Compounds[a]

compd	type[b]	Sn($4d_{5/2}$)	S($2p_{3/2}$)	Se($3p_{3/2}$)	Co($2p_{3/2}$)	C(1s)
SnS_2	i	25.3	161.4			
	ii	25.3 (90)	161.4		781.9 (66)	285.0
		24.0 (10)			779.7 (34)	
$SnS_{1.7}Se_{0.3}$	i	25.2	160.9	159.2		
	ii	25.2 (91)	160.7	159.2	781.9 (41)	284.9
		24.0 (9)			780.0 (30)	
					778.3 (29)	
$SnS_{1.5}Se_{0.5}$	i	25.1	161.1	159.2		
	ii	24.9 (89)	161.2	159.2	781.7 (39)	284.8
		24.0 (11)			779.9 (32)	
					778.2 (29)	
$SnS_{0.7}Se_{1.3}$	i	25.0	161.2	159.9		
	ii	24.9 (89)	161.2	159.8	781.5 (56)	284.9
		23.8 (11)			779.8 (25)	
					778.9 (19)	
$SnS_{0.2}Se_{1.8}$	i	24.7	160.8	159.7		
	ii	24.7 (89)	160.9	159.6	781.8 (58)	284.8
		23.5 (11)			780.0 (25)	
					778.8 (18)	
$SnSe_2$	i	24.6		159.5		
	ii	24.6 (88)		159.6	781.6 (65)	284.8
		23.6 (12)			780.2 (21)	
					779.0 (14)	

[a] Parenthesized numbers represent the percentage of each component present. [b] i = host; ii = intercalate.

Results and Discussion

The intercalation of $CoCp_2$ into single crystals of n-type $SnS_{2-x}Se_x$ (x = 0, 0.3, 0.5, 1.3, 1.85, 2), successfully grown by the I_2 vapor transport method, has been achieved in a solvent medium (CH_3CN) at ca. 65 °C. Table I summarizes the growth conditions, appearance, and *c* spacing of the host crystals, whereas Table II summarizes the reaction conditions, stoichiometry, *c* spacing, and appearance of the intercalates. The rate of reaction markedly decreases as the selenium content of the host crystals increases (Table II), since the weak van der Waals forces holding the layers together are expected to increase in magnitude. A great increase would be expected in the activation barrier to intercalation, which involves prizing the host layers apart to admit a large organometallic species. Accordingly, to ensure complete penetration of $CoCp_2$ into the middle of the host crystals, they were cut up as small as possible (ca. 2 mm × 4 mm). Table II also shows the rate of reaction for the powdered hosts SnS_2 and $SnSe_2$ for comparison.

The host and intercalate powder diffraction spectra consist of a series of (00*l*) lines. Table II gives the characteristic lattice expansion observed for each intercalation reaction, in agreement with other studies of cobaltocene intercalation.[3] The complete set of powder diffraction data can be found elsewhere.[16] A detailed study of the X-ray diffraction spectra of the intercalates has provided detailed information relating to the orientation of cobaltocene molecules between the host layers.[17]

The insulating character of intrinsic SnS_2 prevents the measurement of UPS spectra, since the charge developed on the sample upon ultraviolet irradiation is unable to leak away to earth. Therefore, SnS_2 is doped with phosphorus to increase its conductivity in order to avoid such charging problems. It was deemed wise to dope all members of the host series in an identical manner, despite the more highly conducting nature of the intrinsic selenium-rich hosts.

X-ray Photoelectron Spectroscopy. The crystals of the host and intercalate materials were considered to be of high quality, as previously mentioned.

The binding energy (eV) values of the core levels for the $SnS_{2-x}Se_x$ and $SnS_{2-x}Se_x(CoCp_2)_{0.33}$ crystals are given in Table

(12) Benes, L.; Votinsky, J.; Lostak, P.; Kalousova, J.; Klikorka, J. *Phys. Status Solidi* **1985**, *89*, K1.
(13) Votinsky, J.; Benes, L.; Kalousova, J.; Lostak, P.; Klikorka, J. *Chem. Pap.* **1989**, *42*, 133.
(14) Al-Alamy, F. A. S.; Balchin, A. A. *J. Cryst. Growth* **1977**, *38*, 221.
(15) Cheetham, A. K.; Skarnulis, A. J. *Anal. Chem.* **1981**, *53*, 1060.
(16) FitzGerald, E. T. Thesis, University of Oxford, 1989; Part II.
(17) Ellis, J. Thesis, University of Oxford, **1989**; Part II.

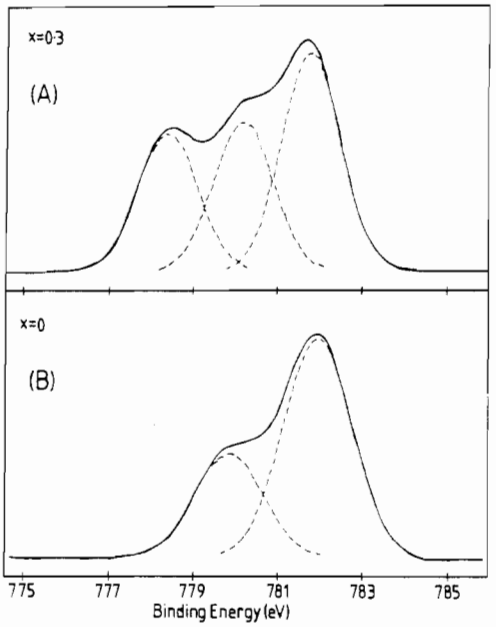

Figure 1. XPS $Co(2p_{3/2})$ binding energy region of the intercalates (A) $SnS_{1.7}Se_{0.3}(CoCp_2)_{0.31}$ and (B) $SnS_2(CoCp_2)_{0.31}$).

III, as well as the relative proportions of the various species present. As a consequence of intercalation, there may be a shift of the Fermi level (E_F) within the band gap, which must be taken into consideration in the interpretation of the XPS results. The main emission peaks due to Sn, S, and Se all remain essentially unchanged upon intercalation, retaining similar binding energies accompanied by a small increase in peak widths. However, for Sn(4d) emission a weak shoulder appears at lower binding energy to the main peak for all members of the series. By fitting Gaussian line shapes to the Sn(4d) peak, it was possible to calculate that the additional species has roughly 10% of the intensity of the main peak for the disulfide case, rising gradually through the series to roughly 12% of the main peak intensity for the diselenide case. Other techniques such as ^{119}Sn Mössbauer spectroscopy could give a second estimate for the degree of tin reduction to compare with these XPS results.

Nevertheless, the data presented are consistent with the formation of a reduced tin species as a result of electron transfer from the $CoCp_2$ molecule. The binding energy separation of the two species (ΔE_B = 1 eV) is constant as the selenium content changes. Similar binding energy shifts have been obtained for the intercalation of Cu into SnS_2[18] and Ag into $SnSe_2$.[19] It might be expected that a two-electron reduction of the tin site is occurring, leading to the formation of a Sn(II) species.[11] Consequently, two cobaltocene molecules are required to effect the complete reduction of a Sn(IV) site.

Figure 1 gives the $Co(2p_{3/2})$ emission peaks for the SnS_2 and $SnS_{1.7}Se_{0.3}$ intercalates. Tables III shows that there appear to be at least two components at approximately 780- and 782-eV binding energy in all cases. The binding energy separation (ΔE_B = 1.8 eV) suggests that the two cobalt species are Co^{2+} and Co^{3+}. The Co^{2+}:Co^{3+} ratio varies between 1:1.3 and 1:3.1 across the series. The XPS spectra of $CoCp_2$ and $[CoCp_2]^+[PF_6]^-$ were recorded in a previous study, which suggested that in SnS_2-$(CoCp_2)_{0.33}$ the two cobalt peaks represent two organocobalt species.[11] The results provide good evidence for the presence of both $CoCp_2$ and $[CoCp_2]^+$ between the layers in the $SnS_{2-x}Se_x$-$(CoCp_2)_{0.33}$ series. Recent ESR studies on $CdPS_3(CoCp_2)_{0.8}$ also demonstrate the equilibrium of these neutral and ionized guest species between the layers.[20]

(18) Ohuchi, F. S.; Jaegermann, W.; Parkinson, B. A. *Surf. Sci.* **1988**, *194*, L69.
(19) Formstone, C. A.; FitzGerald, E. T.; Foord, J. S.; Cox, P. A. *Surf. Sci.*, in press.
(20) Kim, K.; Liddle, D. J.; Cleary, D. A. Personal communication.

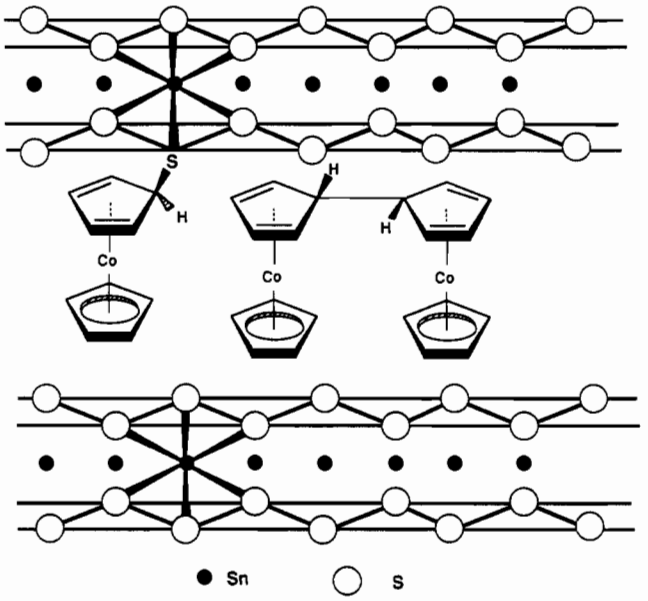

Figure 2. Representation of the possible Co(I) organocobalt species between the SnX_2 layers.

However, a third cobalt species is observed in the XPS spectrum at lower binding energy for all the selenium-containing intercalates ($x \neq 0$) (Table III, Figure 1). Table III demonstrates that this third cobalt species is most prominent at $x = 0.3$ and $x = 0.5$ but gradually diminishes as the selenium content rises further. The shift to lower binding energy indicates a reduction of cobaltocene, but the identity of the reduced species has not yet been unambiguously determined.

Decomposition products such as $CoS_{1-x}Se_x$ and Co metal cannot be ruled out, but these seem unlikely, given the mild reaction conditions. The formation of a distinct surface species is possible, but this can be discounted on the evidence of angle-resolved XPS measurements in which the relative intensities of the three cobalt emissions did not change. The reduction of $CoCp_2$ to $[CoCp_2]^-$ within the intercalates would also appear unlikely, since in order to obtain charge neutrality when roughly 10% of Sn(IV) sites are reduced to Sn(II), only a neutral third cobalt species is permisssible (Table III).

However, it is believed that the unassigned cobalt emission may arise from nucleophilic attack on the cyclopentadienyl ring of $[CoCp_2]^+$ by S^{2-} within the layers to give a neutral $Co(\eta^5$-$Cp)(\eta^4$-diene) complex as shown in Figure 2. This would give a change in the cobalt oxidation state from Co(III) to Co(I), which would be in agreement with the experimental findings. The fact that this effect is not observed in pure SnS_2 may be due to the sulfide layer being insufficiently nucleophilic. As the selenium content of the hosts increases, the sulfur atoms would become more electron-rich and consequently more nucleophilic. The third cobalt species is aso present in the pure $SnSe_2$ case, suggesting that the selenium atoms may function as a nucleophilic entity as well in the sulfur-deficient intercalates.

Table III gives the relative proportions of the various tin and cobalt oxidation states present in these intercalates as determined by XPS. Clearly, there must be sufficient Co(II) to Co(III) oxidation in order to furnish the electrons required to produce the necessary degree of Sn(IV) to Sn(II) reduction. The cationic $[CoCp_2]^+$ and the neutral $Co(\eta^5$-$Cp)(\eta^4$-diene) are both "18-electron" organometallic complexes, so any putative chemical attack by the S^{2-} nucleophile on the $[CoCp_2]^+$ complex can be viewed as a simple rearrangement of electrons in the "guest–host" intercalate system. Therefore, the process of electron transfer from cobalt to tin may be considered to be virtually independent of any postulated nucleophilic attack by S^{2-} on the $[CoCp_2]^+$ complex. Thus, the number of electrons available to reduce the tin sites may be thought to be equal to the sum of the Co(I) and Co(III) species present in the intercalates, given that the Co(I) state is thought to be derived from the Co(III) state. Notice that the {Co(I) +

Table IV. Binding Energy (eV) Data for the He I and He II UPS Spectra Obtained in This Study[a]

compd	type	emission a	b	c	d	e	f[b]
SnS_2	i		3.2	4.9	6.2	8.2	13.9[b]
			(23)	(19)	(11)	(5)	(10)
	ii	2.2	3.4	5.7	8.6	13.1[b]	17.8[b]
		(0.8)	(13)	(45)	(71)	(6)	(8)
	ii	2.3	4.0	5.8	9.0	13.1[b]	17.7[b]
$SnS_{1.7}Se_{0.3}$	i		3.2	5.6	6.9	8.1	13.8[b]
			(22)	(23)	(16)	(12)	(8)
	ii	1.9	3.2	5.6	8.4	12.9[b]	17.7[b]
		(1.0)	(10)	(37)	(77)	(3)	(10)
	iii	2.1	4.4	6.1	8.7	13.0[b]	17.6[b]
$SnS_{1.5}Se_{0.5}$	i		3.0	5.4	6.5	8.1	13.3[b]
			(25)	(19)	(19)	(14)	(8)
	ii	1.5	2.9	5.6	8.4	13.3[b]	17.6[b]
		(1.0)	(10)	(57)	(100)	(2)	(8)
	iii	1.7	3.9	6.0	8.7	13.4[b]	17.6[b]
$SnS_{0.7}Se_{1.3}$	i		2.8	5.0	6.0	8.1	13.4[b]
			(25)	(16)	(16)	(16)	(10)
	ii	1.3	3.2	5.6	8.0	13.2[b]	17.9[b]
		(0.6)	(11)	(35)	(84)	(2)	(5)
	iii	1.6	3.8	5.8	8.5	13.3[b]	17.7[b]
$SnS_{0.2}Se_{1.8}$	i		2.3	4.0	5.4	8.0	13.5[b]
			(26)	(18)	(18)	(14)	(12)
	ii	0–0.4	2.7	5.9	8.8	13.3[b]	17.8[b]
		(0.4)	(10)	(37)	(90)	(4)	(8)
	iii	0–0.3	3.8	5.8	9.0	13.1[b]	17.7[b]
$SnSe_2$	i		2.2	3.9	5.1	8.0	13.8[b]
			(32)	(15)	(13)	(9)	(10)
	ii	0–0.5	2.6	5.9	8.8	13.6[b]	17.7[b]
		(0.6)	(16)	(40)	(69)	(4)	(9)
	iii	0–0.3	3.7	6.4	9.1	13.2[b]	17.6[b]

[a] The host (i), intercalate (ii), and intercalate–host difference (iii) spectral values are presented for each stoichiometry. Parenthesized numbers represent relative intensities of the features. [b] He II data.

Co(III)}:{Co(II)} ratio (see Table III) steadily increases from 2:1 to 3:1, approximately moving from the pure disulfide ($x = 0$) to the pure diselenide ($x = 2$). This agrees very well with an increase in the degree of tin reduction from 10% to 12% across the series in the same direction, assuming a two-electron reduction process. Such considerations enable one to justify the relative proportions of the tin and cobalt species in terms of the electron-transfer process that is taking place.

Evidence for such a model might be expected to come from S(2p) XPS data. However, no significant changes are observed in this core-level emission. In fact, the Se(3p) and S(2p) emissions are to be found in the same binding energy region. This makes Gaussian fitting the XPS data rather difficult, and consequently any subtle changes in the photoemission peaks might be obscured. The $SnS_{1.7}Se_{0.3}(CoCp_2)_{0.31}$ case might be expected to give the most obvious modification to the S(2p) emission relative to the SnS_2 intercalate, since the third cobalt species is most prominent in this instance. However, even in this intercalate, in which roughly 5% of the sulfur atoms would be associated with a nucleophilic attack, no significant change can be observed in the available S(2p) XPS data. The problems in analyzing the S(2p) XPS data are probably made more acute by the unmonochromated nature of the X-ray radiation.

Thus, although the proposition of a nucleophilic attack to explain the third cobalt species has its attractions, it is clear that there are still some objections to it to be overcome.

Another possibility to be considered is that pairs of neutral cobaltocene molecules are reductively coupled between the layers[21] to give a dicobalt complex as shown in Figure 2. This would give rise to a Co(II) to Co(I) reduction. The analogous rhodocene dimerization complex has previously been characterized.[22]

(21) Bercaw, J. E. Personal communication.
(22) El Murr, N.; Sheats, J. E.; Geiger, W. E., Jr.; Holloway, J. D. L. *Inorg. Chem.* **1979**, *18*, 1443.

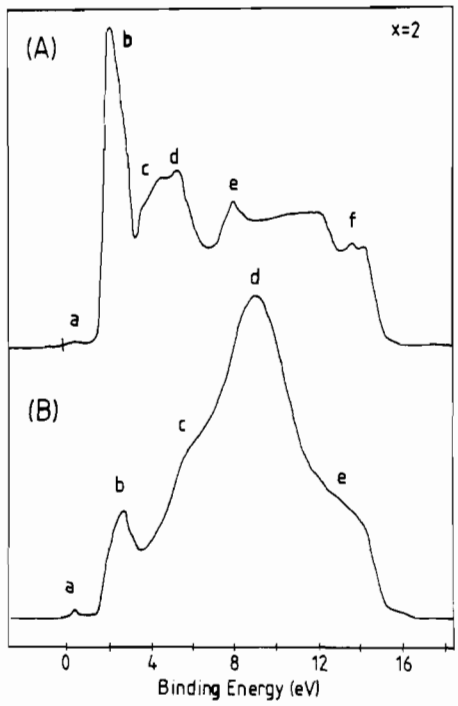

Figure 3. He I UPS spectra of (A) $SnSe_2$ and (B) $SnSe_2(CoCp_2)_{0.33}$.

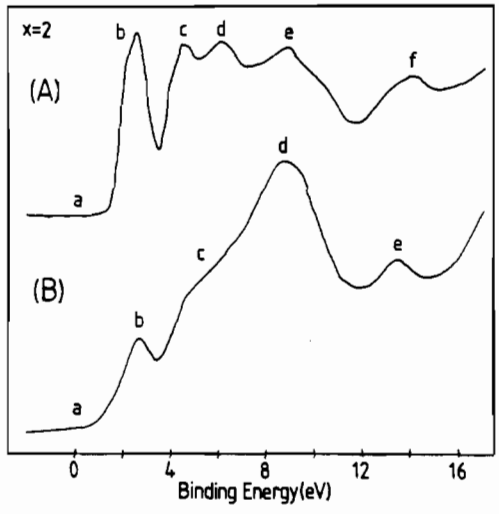

Figure 4. He II UPS spectra of (A) $SnSe_2$ and (B) $SnSe_2(CoCp_2)_{0.33}$.

Finally, the Co:Sn ratio was determined to be in the range 0.3–0.5 by XPS, in rough agreement with chemical analysis, though a cobalt-rich surface layer would account for Co:Sn being greater than expected. The Co:C ratio was ~1:10 for all the intercalates. The S:Se ratio from XPS was roughly as expected from the crystal stoichiometries.

Ultraviolet Photoelectron Spectroscopy. The valence-band spectra of the host and intercalate surfaces will not be presented in full, since the host spectra all look similar, as do the intercalate spectra. Table IV summarizes the binding energy and relative intensity data for the main features of the valence-band spectra for the host (i) and intercalate (ii) surfaces, as well as the binding energies alone of features in the (intercalate–host) difference spectra (iii). The derivation of the difference spectra will be explained shortly. The intensity data were obtained by removing a rising background from the spectra and estimating as best as possible by square-counting the areas beneath features. The labels a–f in Table IV represent different emissions in each of the cases (i), (ii), and (iii). He I UPS provides the main data, while He II UPS gives additional data at higher binding energy values.

The host UPS spectra (Table IV) show emissions (b–f) that corresponds to the bands formed by the overlap of Sn(5s,5p), S(3s,3p), and Se(4s,4p) orbitals.[23,24] To take a specific case,

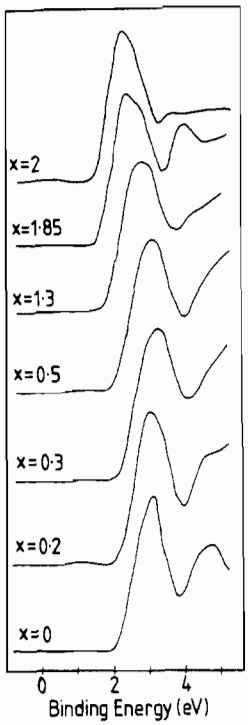

Figure 5. He I UPS spectra of the host crystals in the binding energy region 0–5 eV.

Figures 3A and 4A show the He I and He II UPS spectra of $SnSe_2$. In general, the peaks (b–e) at BE = 2.2–3.2, 3.9–4.9, 5.1–6.1, and 8.0 eV are derived from S(3p) and/or Se(4p) orbitals, whereas the feature at roughly 13.6-eV binding energy (peak f) is derived from S(3s) and/or Se(4s) orbitals. UPS indicates that each host is an n-type semiconductor, the valence-band maximum (VBM) shifting to lower binding energy as the selenium content increases, consistent with the decreasing band gap of the host, as demonstrated in Figure 5. The phosphorus doping may lead to n-type behavior in all cases, with the Fermi level pinned just below the conduction band. The emission in the host band gap (peak a) for all the host stoichiometries arises from He Iβ satellite excitation of the intense VBM. Helium-discharge lamps give He Iα (21.22 eV) and He Iβ (23.09 eV) emissions with a relative intensity 100:1.7. The He II spectra do not suffer from such spurious features in the band gap, since the He IIβ satellite excitation is roughly 8 eV higher in energy than that of He IIα.

The intercalate He I,II UPS spectra (Table IV) all show characteristic emissions (a–f) at BE = 0.0–2.0, 3.0, 6.0, 8.5, 13.1, and 17.8 eV. Figures 3B and 4B show the $SnSe_2(CoCp_2)_{0.33}$ He I and He II spectra, where the emissions (a–e) are labeled.

In each case, there is a dramatic change upon intercalation, although the intercalate spectra are broadly similar across the series. The broad emission (b) at ca. 3.0-eV binding energy, which has been shifted and attenuated by movement of the Fermi level (E_F) within the band gap upon intercalation, represents the residual contribution from the chalcogen np σ band (host VBM). The other emissions (c–f) are due to the guest molecules, though the additional intensity in the band gap (peak a) stems from the transfer of electrons onto the tin atoms.

The changes taking place upon intercalation are better understood by considering a difference of the intercalate and host valence-band emissions, the so-called "difference spectrum". It might be thought that taking the difference between two such dissimilar spectra might cause problems. In order to make the difference spectrum in each case as meaningful as possible, a normalization process was undertaken prior to subtraction. The VBM of the host emission (Figure 3A, peak b) is attenuated strongly upon cobaltocene intercalation to give a corresponding feature in the intercalate emission (Figure 3B, peak b). By normalizing these two corresponding features in the host and intercalate spectra, the subtraction process was deemed to be more satisfactory than otherwise. Emissions in the band gap of the host and intercalate spectra, a result of He Iβ satellite excitation of the VBM in each case, would be expected to cancel approximately by using this method of data analysis. This method has been used in other studies[8,11] to show very clearly the effects of intercalation on the electronic structure of layered materials, especially in the band gap region near the Fermi level (E_F).

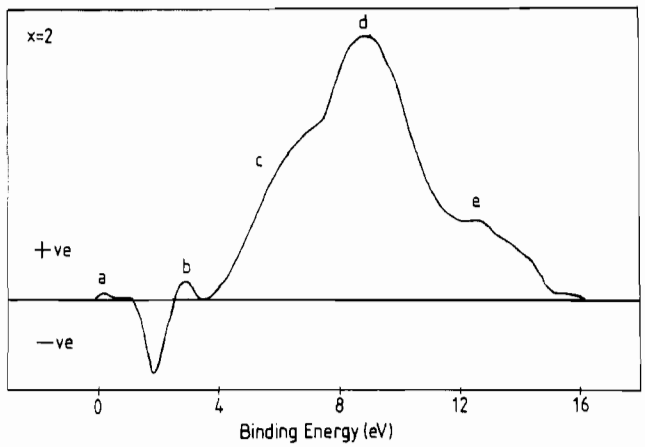

Figure 6. He I UPS difference spectrum (intercalate–host) for the diselenide case.

When calculated for all members of the series, these difference spectra show characteristic broad emissions (a–f) at BE = 0.0–2.3, 3.8, 6.0, 8.7, 13.1, and 17.6 eV (Table IV). Figure 6 shows the specific difference spectrum for the diselenide case. The difference spectra represent the emissions from the three intercalated cobalt species as well as the new states (peak a) formed in the band gap by electron transfer. It has been shown that the XPS valence-band difference spectrum of the disulfide case was very similar to a weighted summation of the corresponding $CoCp_2$ and $[CoCp_2]^+[PF_6]^-$ spectra.[11] The analogous demonstration by UPS was not possible, since these organometallic materials are insulating in character.

The emission peaks (b, c) in the binding energy range of ca. 3–7 eV can be assigned to Co 3d states, whereas the peaks (d, e) in the range ca. 9–13 eV can be assigned to η-Cp π-bonding states. This is in agreement with the gas-phase UPS data on cobaltocene molecules.[25]

The difference spectra show that additional states have appeared in the band gap upon intercalation. Figure 7 represents the narrow-scan (0.5-eV binding energy region) difference spectra for the series, which demonstrate that the maximum of the band gap emission shifts closer to the Fermi level (E_F) as the selenium content increases. The emission tails off toward E_F in all the cases. However, in the selenium-rich cases (x = 1.85, 2) the density of states at E_F is nonzero, indicating that these materials are metallic, whereas the other materials (x = 0, 0.3, 0.5, 1.3) are small band gap semiconductors. Conductivity measurements have recently confirmed this spectroscopic assessment.[26]

The band gap emission would be expected to be partially associated with HOMO Co dπ^* states of neutral $CoCp_2$ molecules between the layers, but new states may have formed as a result of electron transfer from Co dπ^* donor orbitals into Sn(5s,5p) acceptor orbitals. This view is reinforced by the XPS results presented earlier showing reduction of the tin sites and oxidation of the cobalt sites. The "s"-like character of the tin acceptor states is clear from the significant loss of the conduction band intensity

(23) Shepherd, F. R.; Williams, P. M. *J. Phys. C* **1974**, *7*, 4416.
(24) Lee, P. A., Ed. *Physics and Chemistry of Materials with Layered Structure*; D. Reidel: Dordrecht, The Netherlands, 1976, Vol. 4, p 273.
(25) Cauletti, C.; Green, J. C.; Kelly, M. R.; Powell, P.; Van Tilborg, J.; Robbins, J.; Smart, J. *J. Electron Spectrosc. Relat. Phenom.* **1980**, *19*, 327.
(26) Formstone, C. A.; FitzGerald, E. T.; O'Hare, D.; Cox, P. A.; Kurmoo, M.; Hodby, J. W.; Lillicrap, D.; Goss-Custard, M. *J. Chem. Soc., Chem. Commun.* **1990**, *6*, 501.

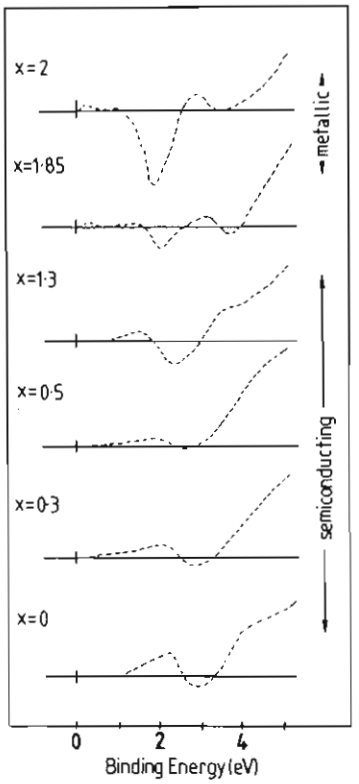

Figure 7. He I UPS difference spectra in the binding energy region 0–5 eV for the entire series.

going from He I to He II excitation as in Figures 3 and 4.

The negative intensity in the difference spectra (Figures 6 and 7) is caused by the shift of the host VBM upon intercalation, as a result of the movement of the Fermi level (E_F) within the band gap, leading to a mismatch at ca. 3.0 eV upon subtraction of the host data from the intercalate data. As previously mentioned, despite this problem in subtracting such dissimilar spectra, this data analysis technique is thought to give a valid demonstration of new states forming near the Fermi level.

The difference spectrum (intercalate–host) and intercalate spectrum in each case are alike, so it appears that the intercalate spectrum represents mainly the cobaltocene emission with the host emission greatly attenuated. UPS is surface sensitive (escape depth ca. 2 nm), and therefore it is likely that organocobalt species constitute the uppermost layer of the surface. This view is supported by the decrease of ca. 1 V in the surface work function upon intercalating the host crystals, pointing to a positively charged metallocene overlayer.

Impurity-Band Model. A qualitative band model description would be useful in understanding the process of electron transfer between the guest and the host. A rigid band model approach[8] would view the intercalate band structure as the sum of the guest and host valence bands (VB's) together with the creation of a partially filled conduction band (CB) by electron transfer. However, the observed changes near the Fermi level (Figures 6 and 7) suggest that the process of electron transfer does not simply fill the empty Sn(5s,5p) states in the conduction band to give a metallic system in all cases. The evidence indicates that there are strong electron-localizing effects at play, especially in the sulfur-rich intercalates (x = 0.0, 0.3, 0.5), so that simple band theory is inapplicable.

The impurity-band model for heavily doped semiconductors (e.g. P/Si) offers a useful approach to the understanding of the intercalate electronic structure. The overlap of the impurity orbitals is significant at high impurity concentrations, resulting in the formation of an impurity band close to the conduction band of the semiconductor, as in Figure 8. However, metallic conductivity does not follow directly, since the localizing effects of the impurity potential may be significant. The Hubbard criterion states that the width of the impurity band (W) must be greater than the

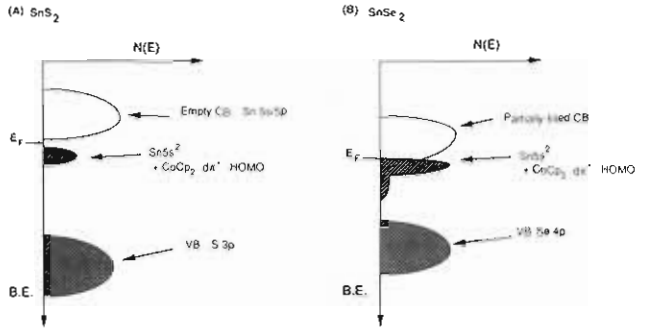

Figure 8. Schematic band structure diagrams for the cobaltocene intercalates of (A) SnS_2 and (B) $SnSe_2$.

electron repulsion (U) in a band, in order that a delocalized metallic system can form. Indeed, at a critical impurity concentration, the doped system may become metallic.

The substitutional nature of the doping in P/Si is clearly distinct from the reaction that intercalates $CoCp_2$ into SnX_2 hosts, but the guest species can be considered to be an impurity sitting adjacent to the acceptor tin sites. The electron transfer is viewed as an overlap of empty Sn(5s,5p) states, with the filled $CoCp_2$ $d\pi^*$ impurity states leading to the formation of an impurity band near the host conduction band. The transfer of an electron onto a Sn(IV) site creates a strong electron–phonon interaction, such that a second transferred electron gives a Sn(II) valency; Sn(III) is commonly observed to disproportionate. The Sn $5s^2$ states that constitute the impurity band form below the main empty conduction band states (Figure 8). The parent $[CoCp_2]^+$ attractive potential adjacent to the reduced tin site tends to localize the electrons as well. Thus, these mixed-valency materials may be pictured as having electrons hopping between the tin and cobaltocene sites. XPS is able to detect two tin oxidation states, the hopping being slow on an XPS time scale.

For $SnS_2(CoCp_2)_{0.33}$ the effects of the lattice distortion at the tin site and the $[CoCp_2]^+$ impurity potential may be sufficient to localize the transferred electrons into an impurity band in the band gap (Figure 8A). Conductivity studies have confirmed the semiconducting character of the disulfide intercalate.[11]

The impurity band width (W) depends on the impurity concentration (n_d) and the width of the host conduction band. The electron repulsion energy (U) depends on the size of the impurity orbitals (Sn $5s^2$), which is directly related to the polarizability of the medium, i.e. the screening of the ionized electrons from $[CoCp_2]^+$ by the medium. Treating the impurity orbitals as hydrogenic with radius a_H, Mott deduced that the transition to the metallic state, as the electron repulsion effects within the impurity band are overcome, is achieved at $n_d^{1/3}a_H \sim 0.25$.[27]

As the sulfur is replaced by selenium in the intercalates, the bandwidth of the host conduction band increases and the polarizability of the medium increases, but the impurity concentration remains constant (Sn:Co ~ 3:1). Thus, the extent of Sn(5s,5p) and $CoCp_2$ $d\pi^*$ overlap increases to give a shift of the impurity band, eventually giving an extended overlap with the host conduction band such that a transition to metallic behavior at a critical selenium content ($1.3 < x < 1.85$) occurs. Figure 8B represents the band structure for the diselenide case. The electrons on the reduced tin sites may now be to some extent itinerant in the impurity band. Conductivity measurements on $SnSe_2(CoCp_2)_{0.33}$ confirm the metallic character of this material and reveal that it is a type II superconductor.[26]

However, XPS reveals two tin emissions in all cases, which would normally indicate mixed valency. Indeed, for the disulfide case, Mössbauer spectroscopy has confirmed this hypothesis.[11] Final-state effects in XPS could also account for such doublets, although non-transition-metal compounds are unlikely to produce this complication.[28] Thus, despite the lack of Mössbauer mea-

(27) Edwards, P. P.; Sienko, M. J. *J. Am. Chem. Soc.* **1981**, *103*, 2967.
(28) Chazalviel, J. N.; Campagna, M.; Wertheim, G. K. *Phys. Rev. B* **1977**, *16*, 697.

surements, the metallic intercalates (x = 1.85, 2) appear to be mixed-valency compounds. The impurity band (Sn $5s^2$) probably consists of a few delocalized states near the Fermi level, whereas the states near the bottom of the band are still under the localizing influence of the parent $[CoCp_2]^+$ potential.

Finally, the neutral cobaltocene species must contribute HOMO Co($3d\pi^*$) states in the band gap overlapping with the main Sn $5s^2$ impurity band (Figure 8).

Conclusion

The intercalation of cobaltocene into the single crystals of the layered tin dichalcogenides $SnS_{2-x}Se_x$ has presented the opportunity to study the electronic structure changes taking place by using photoelectron spectroscopy. For this work it was essential to prepare single crystals, which can be cleaved in UHV to give clean, undisturbed surfaces. The systematic variation of the sulfur and selenium content of these materials has produced an interesting variation in physical properties through the intercalate series.

The XPS core-level studies have shown that both the tin and cobalt species exhibit mixed oxidation states throughout the series. This observation has been taken as evidence that electron transfer is occurring between the guest and host entities upon intercalation. Intercalation of other guest molecules such as ferrocene ($FeCp_2$) and chromocene ($CrCp_2$) into the SnS_2 host has previously been attempted.[11] The lack of success in the disulfide case has not been followed up in the selenium-containing hosts. However, attempts at intercalation of these guest molecules could be worthwhile, since, if successful, this would test the hypothesis that ferrocene (less reducing than cobaltocene) would give less extensive electron transfer to the tin sites, while chromocene (more reducing than cobaltocene) would give a greater degree of electron transfer. The intercalation of the $Co(C_5Me_5)_2$ molecule into the $SnS_{2-x}Se_x$ hosts might present a possibility of investigating the nature of the postulated nucleophilic attack on the guest molecule. However, in the SnS_2 instance, it is not possible to intercalate the $Co(C_5Me_5)_2$ molecule.[11]

The valence-band study using UPS has demonstrated that the electron transfer has created new states in the band gap of the intercalates. Increasing the selenium content of the intercalates results in a transition from semiconducting to metallic behavior. The polarizability of the medium has been postulated as the crucial factor determining the nature of the states formed in the band gap upon intercalation.

The results of PES show clearly that the host properties have a great influence on the nature of the intercalated guest species and the overall electronic structure of these intercalated materials. Recent observations of superconductivity in these metallic intercalates[26] has given impetus to further work, which will concentrate on other physical measurements and the possibility of intercalating other guest molecules into these layered structures.

Contribution from the Departments of Chemistry, University Center at Binghamton, State University of New York, P.O. Box 6000, Binghamton, New York 13902-6000, and University of Southern California, Los Angeles, California 90089

Photophysical Studies of $W(CO)_5L$ Complexes. Multiple-State Luminescence of $W(CO)_5$(4-cyanopyridine) in Fluid and Glassy Solutions

Kathleen A. Rawlins,[†] Alistair J. Lees,*[,†] and Arthur W. Adamson[‡]

Received February 14, 1990

Electronic absorption spectra, luminescence spectra, excitation data, and luminescence lifetimes have been recorded from $W(CO)_5$(4-CNpy) and $W(CO)_5$(pip) (4-CNpy = 4-cyanopyridine; pip = piperidine) complexes in methylcyclohexane solutions at 210–313 K and in EPA glasses at 77 K. The results illustrate that $W(CO)_5$(4-CNpy) is a multiple-state emitter displaying dual emission bands at any of the measured temperatures; the emitting levels are assigned to metal to ligand charge-transfer (MLCT) excited states that are predominantly of triplet character. In fluid solution the two ^{3}MLCT emitting levels establish a thermal equilibrium and the luminescence data obtained from temperatures between 210 and 313 K can be fitted to a modified Boltzmann model yielding an energy separation between the participating states of 990 (±50) cm^{-1}. In a frozen glass the two radiative ^{3}MLCT excited states are no longer thermally equilibrated, as evidenced by their different emission lifetime values and by an excitation wavelength dependence in the emission spectra. Luminescence spectra and lifetimes have also been observed from $W(CO)_5$(pip) at low temperature, and its emitting level is assigned to a ligand field (LF) state of predominantly triplet character. No evidence has been obtained for a ^{3}LF radiative route in $W(CO)_5$(4-CNpy), even at 77 K; this result, taken in conjunction with prior photochemical studies, indicates that although the LF levels are effectively populated on near-UV light excitation, they undergo very efficient radiationless deactivation, including conversion to the emitting ^{3}MLCT excited-state manifold.

Introduction

Photophysical studies of transition-metal organometallic complexes are essential in determining and characterizing their lowest lying electronically excited states. In several metal complex systems, luminescence techniques have been used most successfully as spectroscopic probes to provide valuable insight into the nature of their often intricate excited-state levels and deactivation pathways.[1]

The $W(CO)_5L$ (L = a substituted pyridine) system is of special significance because these complexes were the first 6 metal carbonyls observed to luminescence in frozen glasses[2] and in fluid solution.[3] Indeed, their electronically excited states are among the longest lived determined to date for group 6 metal carbonyl systems, exhibiting emission lifetimes of over 400 ns in room-temperature solution.[1,3b] Despite this knowledge, a number of aspects concerning their photophysical properties remain to be understood. Specifically, although these molecules are known to possess two lowest energy metal to ligand charge-transfer (MLCT) transitions and a proximate ligand field (LF) transition,[4] the exact role of these states in the photophysical deactivation mechanism is not clear. The earlier published photophysical work[3b] clearly implicated the presence of two close-lying MLCT excited levels

[†]SUNY.
[‡]USC.

(1) Lees, A. J. *Chem. Rev.* **1987**, *87*, 711 and references therein.
(2) (a) Wrighton, M.; Hammond, G. S.; Gray, H. B. *J. Am. Chem. Soc.* **1971**, *93*, 4336. (b) Wrighton, M.; Hammond, G. S.; Gray, H. B. *Inorg. Chem.* **1972**, *11*, 3122. (c) Wrighton, M.; Hammond, G. S.; Gray, H. B. *Mol. Photochem.* **1973**, *5*, 179. (d) Wrighton, M. S.; Abrahamson, H. B.; Morse, D. L. *J. Am. Chem. Soc.* **1976**, *98*, 4105.
(3) (a) Lees, A. J.; Adamson, A. W. *J. Am. Chem. Soc.* **1980**, *102*, 6874. (b) Lees, A. J.; Adamson, A. W. *J. Am. Chem. Soc.* **1982**, *104*, 3804.
(4) Geoffroy, G. L.; Wrighton, M. S. *Organometallic Photochemistry*; Academic: New York, 1979 (and references therein).

0020-1669/90/1329-3866$02.50/0